Crystal plasticity of Cu nanocrystals during collision

Bingqing Cheng[§] and Alfonso H.W. Ngan

Department of Mechanical Engineering, The University of Hong Kong, Pokfulam Road, Hong Kong, P.R. China

[§] Correspondence author (email: tonicbq@gmail.com)

Abstract

In this work, we simulate the response of two Cu nanoparticles colliding at different approaching rates at room temperature by MD. For small nanospheres, the formation of single twins is favored at high approach rates, whereas larger nanospheres mainly deform by dislocation slip. For small nanocubes with large {100} flat surfaces, however, a dislocation-free direct geometrical conversion process that leads to five-fold twinning dominates except at highly retarded approaching rates. For larger nanocubes, single twin formation is the governing plasticity mechanism. The probability for plastic deformation by dislocation slip or twinning is attributed to the abundance of surface steps, which act as sites for dislocation nucleation.

Keywords

Nanoparticle, plasticity, dislocation, twinning, shear wave, cold sintering

1. Introduction

The strength and deformation of nano-sized crystals have attracted tremendous attention in recent years, as they exhibit interesting phenomena such as strong size dependence of strength and jerky flow [1-5]. These are due to the fact that dislocations are difficult to be stored inside small crystal volumes, and hence the basic deformation mechanisms are significantly altered from the bulk state[6]. Much of the work performed so far, however, has focused on simple tensile/compressive behavior. Yet, in many technological applications such as gas phase synthesis and sintering, a highly dynamic mode (i.e. collision) also causes deformation of nanoparticles.

At high temperatures, surface diffusion, lattice diffusion from surface, vapor transport, grain boundary diffusion, viscous flow, and amorphous plastic flow constitute the deformation mechanisms in sintering for micro-sized as well as nano-sized particles [7-9]. On the other hand, the impact deformation modes and mechanisms of nanocrystals as they collide with each other at lower temperatures have been a much less investigated subject. This topic is potentially interesting as high stresses exceeding the theoretical strength of the material can be developed at the contact between the interacting particles leading to dislocation slip [10-13]. Furthermore, the stability and hence deformation of nanocrystals are likely to be mediated by free surface effects even at low temperatures, in addition to known effects due to the dislocation starvation condition concluded from nano/micro-pillar compression studies [1]. We have shown recently that at 300K, Cu nanocrystals can coalesce together with the formation of a peculiar type of five-fold twins in the sintered product via an unseen before dislocation-free process involving a series of shear waves and rigid-body rotations[11]. In a separate study[14], we have also shown that such five-fold twinned structures can also be formed by simply heating single Cu nanocrystals, and the transition pathway involved was identified to be another variant of a dislocation-free, shear wave mechanism which we termed "direct geometrical conversion". In this process, a cluster of atoms rearranges in a highly coordinated way between different geometrical configurations (e.g. fcc, decahedral, icosahedral) without involving dislocations. These preliminary studies have shown that the deformation mode and mechanism of nanocrystals can be far from our conventional understanding involving dislocation plasticity alone.

Despite the abovementioned preliminary work, several important issues remain unanswered. First, in addition to five-fold twinning, conventional processes of dislocation slip and twinning via Shockley partial dislocations were also identified during nano-crystal coalescence [11], and it is not clear which process will dominate at a certain condition. Secondly, in our previous study [11], two unsupported Cu nanoparticles were placed within their interaction range and released from rest, and they mutually interacted without any external disturbance. A typical evolution of the distance between their centers of mass is shown in Fig. 1, indicating that the two particles approach and impact on one another rapidly with a relative velocity of approximately ~100 m/s at the initial stage of collision. However, in real situations

such as gas-phase synthesis, the collision or approach speed of particles can be much higher or lower than that under natural interaction condition, depending on factors including the initial particle velocity, surface contamination, drag from surrounding atmosphere, friction from substrate, and so on. It is therefore interesting to see how the deformation depends on the collision strain rate.

In an attempt to address the aforementioned issues, in the present study we simulate the plasticity response of Cu nanoparticles of different shapes colliding at different strain rates by Molecular Dynamics 你. Although MD cannot capture the real time and space scales in a vast majority of physical and technological phenomena, it is fortuitously a very suitable tool for the direct simulation of nanoparticles, because such a problem involves a small enough system size comprising thousands or so atoms, as well as an intrinsically quick process time span, both of which can be handled directly by MD. To investigate the effects of the initial velocities of the particles and the surroundings, we let the two nanoparticles collide into one another at different approaching velocities, by controlling the relative positions of their centers of mass. In this way, we can control the collision strain rate and study how this affects the deformation.

2. Simulation Method

The MD program in use employed the leap-frog formulation with a time step of 2fs. Atoms were allowed to interact through an EAM potential for Cu developed by Sheng, Kramer, Cadien, Fujita and Chen [15]. This potential was found to provide reasonable estimates of the surface energies, as well as stacking fault and twin energies, for Cu [15]. Two individually relaxed single crystalline Cu nanoparticles were allowed to interact for 400 ps (200,000 time steps) at 300K. The [100], [010], [001] lattice directions of the two particles were parallel to the x, y and z axes of the system, respectively, with the two nanoparticles initially aligned along the x axis. The two particles had the same radius ($1nm < R < 5nm$), with either cubic or spherical shapes. Such a choice is to study the effects of cubic faces, which are plenty in the cubic crystal shape but not so in the spheres, and this will become clear later on. The two Cu nanoparticles were made to penetrate into one another at a fixed speed of 10m/s, 50m/s or 200m/s, before a maximum penetration depth of 0.78 nm was reached, after which their centers of mass were kept still. This was done by fixing the centers of mass of the two particles along the designated pathway, thereby involving external forces on the particles. Comparing with Fig. 1 where the approach speed under natural interaction conditions is ~100m/s, the approach speeds chosen here include much smaller and much larger values. The initial distance between the two particles (i.e. the gap between the centers of closest atoms from different particles minus one lattice spacing of {100} planes) was 0.22 nm, and, as said before, the maximum penetration depth was set to be 0.78 nm. For nanoparticles within the given size range, the strain corresponding to such penetration depth is well beyond the elastic limit.

Apart from controlling the penetration rate of the two nanoparticles, the program does not put in place any additional velocity control scheme. The system can therefore be regarded as in a quasi-constant-energy ensemble initially at 300K. The conjugate gradient minimization technique was used to remove thermal noise when determining the crystal structure of the final products.

3. Results

3.1 Spherical nanoparticles

Two spherical nanoparticles of the same shape and size were allowed to penetrate into one another at different rates. After the simulations, the crystal structure of each particle was analyzed. It is found that particle size and penetration speed influence the governing mechanism for the plastic deformation process involved: twinning is favored in small sized particles at high penetration rates, whereas dislocation slip dominates for larger nanoparticles, and direct geometrical conversion is altogether absent (see Table 1).

For nanoparticles with 25125 atoms penetrating at 50m/s, dislocation slip is the identified plastic deformation mechanism. The penetration force and pressure distribution over the contact plane are shown in Figs.2(a,b). The atomic movements during the penetrating process are revealed by relative displacement plots in Fig. 2(c). Here, a thin layer of atoms comprising two adjacent (110) planes of one colliding particle, and crossing the centers of both particles and the contact point, is analyzed. The initial atomic positions are plotted as blue dots. For each nearest-neighbor pair (i, j) of atoms in the plot, their relative displacement r_{ij} is calculated as the displacement of atom i relative to that of atom j. To distinguish the direction of r_{ij}, we define atom i to be always on the right hand side of atom j, or when they have the same horizontal coordinate, atom i to be above atom j. The in-plane component of r_{ij} is represented in both magnitude and direction by a black arrow drawn between each atomic pair. The out-of-plane component of r_{ij} is represented by a vertical red arrow that points upward if this component is out of the paper, and downward otherwise. The relative displacement plots are particularly useful in revealing dislocation slip and twin formation processes. When a perfect or partial dislocation glides on a close packed plane, an array of relative displacement vectors equal to the Burgers vector trails behind the dislocation on the slip plane. The formation of a single twin, on the other hand, is indicated by arrays of displacement vectors equal to the Shockley partial Burgers vector filling up the twinned region. The atoms near the edge of the region of twinning vectors are on the twin boundaries. If five twin boundaries intersect, it means that a fivefold twin has formed.

The penetration lasted for 20 ps before reaching the maximum contact depth of 0.78 nm. It is interesting to relate the penetration force evolution with the dislocation activity depicted in Fig. 2(c). Before 4.4ps, the gap between the surfaces of the two particles is decreasing, and the

load is negative to balance the attraction between the two particles. No dislocation is nucleated at this stage. From 4.4ps to 20ps, a compressive force builds up quickly between the two particles, and dislocation activities begin. Very often, a partial dislocation is nucleated from the surface, which later turns into a perfect dislocation. From 20ps to 30 ps, the force is gradually relaxed, but dislocations are still active. At the end of 30ps, a quite complex dislocation debris network is built, and after that, a small residual force remains in the structure until the end of the simulation, then dislocation activity is muted.

The radial distributions of pressure over the contact plane have a similar profile during penetration: compressive at the center of the contact area and adhesive outside the edge of the neck. The maximum compressive pressure for the present case reaches around 10 GPa, which is far beyond the bulk yielding point (70 MPa) and approaching the theoretical strength of Cu ($\sim E/10 \sim 12$ GPa). Note that the maximum compressive pressures in different simulation cases are generally different. Generally, a larger pressure is correlated with a larger nanosphere and the pressure is almost independent of the penetration rate in our simulations.

Fig. 3 shows a case where twinning is the identified crystal plasticity mechanism. The penetration force evolution is similar to the previous case. In this case, a shorter time span between 20ps and 25ps is required for the force to relax to a small residual value. Due to the small system size, only a very limited amount of data for pressure distribution can be extracted. Still, the compressive force inside the contact area and the tensile peak for adhesion are recognizable during penetration. The displacements of a few atoms near the contact neck seem chaotic. Apart from this, for single twins, we found the emission of Shockley partial dislocations from free surfaces, which glide into the crystal and introduce stacking fault layers. In some simulation cases (see Fig. 4(c)), a thin lamellar of twin or stacking fault is formed first, and this gradually increases in thickness by combining with another stacking fault layer on an adjacent slip plane near the twin boundary. For other cases like that in Fig.3(c), the growth of twin is not always sequential on adjacent close packed planes. Many partial dislocations slip simultaneously in a particular region in the nanoparticle. In Fig. 3(c3), the nanocrystal has accumulated a number of partial dislocations. Afterwards, probably for the minimization of potential energy, the partials are repelled from the crystal, and the structure rearranges to form a single twin and a stacking fault layer.

3.2 Cubic nanoparticles

Another set of simulations was carried out for cubic particles colliding {100} face-on under different strain rates (Table 2). When the cubic nanoparticles are very small, the plastic deformation identified is usually direct geometrical conversion resulting in five-fold twins[14]. For larger cubic nanoparticles, single twinning is the dominating mechanism.

For single twinning, a simulation case with the penetration force evolution, pressure distribution as well as the relative displacement maps is presented in Fig. 4. Before 4.4ps, the adhesion between the two {100} surfaces of the two cubes is quite large, which is due to the flatness of the surfaces. From 8ps to 20ps, compressive force accumulates, and this relaxes very quickly through the twinning events. From the relative displacement maps in Fig. 4(c), emission and accumulation of Shockley partial dislocations also take place from free surfaces at adjacent {111} planes, similar to the case in Fig.3.

For the direct geometrical conversion process (Table 2), a full account has been given in our previous work [14]. In summary, five-fold twins are formed via twinning shear and rigid-body rotation processes, the transmission of which is by shear waves instead of gliding of partial dislocations. The penetration force evolution and pressure distribution plots for the direct geometrical conversion process are quite similar to Fig. 4(a,b) and so are not reproduced here. Fig. 5 shows the shape evolution of the particle during the process, with the final product in Fig. 5(d) being a five-fold twin consisting of {111} surfaces converted from initial {100} surfaces. Notice also the continuous change of the angles between the diagonals during the conversion, and that in the final structure in Fig. 5(d), some of the initial {111} surfaces have transformed into a shallow pyramid of {111} phases. Another interesting feature of the direct geometrical conversion process is that each of the shell layers of the initial cubic crystal buckles to form a corresponding shell layer of the resultant five-fold twin [14].Identification of the five-fold twin structure and the shear-wave, dislocation-free process involved was carried out in a similar fashion involving careful analysis of the relative displacement maps as reported previously [14], and in the interest of space, these intermediate steps are not repeated in here.

3.3 Dislocation slip or twinning?

From the above summary of results, spherical or cubic nanoparticles can deform plastically through three mechanisms at different indentation rates: dislocation slip, single twinning by Shockley partials, and five-fold twinning by direct geometrical conversion. It is interesting to distinguish which factor will favor the occurrence of each possible mechanism.

First, in the present work, direct geometrical conversion only occurred for cubic nanoparticles with small sizes. In our pervious study, by heat treating small-sized nanoparticles, we also found that direct geometrical conversion could happen for cubic and cubotahedral nanoparticles, but was absent for spherical, octahedral and truncated octahedral particles of similar sizes. The transition is probably due to the instability of {100} surfaces relative to {111} – hence a particle with a lot of {100} surfaces, like the present cubic ones, tends to convert itself into a five-fold twinned structure with more {111} surface area (see Fig. 5). The activation energy for the transition was estimated to be several eV, and increases with the particle size. Combining the results from both studies, we conclude that: (i) nanoparticles with a lot of {100}

surface areas are prone to undergo direct geometrical conversion; [16] nanoparticles with small sizes have lower activation energy for the transition, so that the conversion is more likely to happen.

From the results in Tables 1 and 2, it can be concluded that single twinning happens for cubic or small spherical nanoparticles. For larger spherical particles, dislocation slip becomes the dominating deformation mechanism. To gain a deeper understanding, we carefully observed the atomic movements (i.e. relative displacement maps) during the simulations. We discovered that, for all the simulation cases in the present work where dislocation slip is the governing mechanism, perfect dislocations were always nucleated at surface steps. Sometimes a partial dislocation nucleated first and then quickly turned into a perfect dislocation. In other occasions a perfect dislocation nucleated at a free surface directly. We selected several representative cases and plot the relative displacement maps for spherical particles to depict the first nucleation event in Fig. 6(a-c).To further support this claim, we carried out several trial simulations for cuboctahedral and truncated octahedral nanoparticles with various sizes under different strain rates. Yet all the dislocations were nucleated from sharp edges, which operate similarly to a step on the surface.

For cubic nanoparticles being collided on along their [100] lattice direction, the (100) surface under compression is atomically flat. On the contrary, the surfaces of spherical particles are built from different layers of atoms, and therefore have an abundant number of steps. In this way, it has become clear why dislocation slip was suppressed when cubic nanoparticles collide {100} face-on, as there are no surface steps on {100} faces.

Another observation from Fig. 6 is that, new dislocations are nearly always nucleated at the step closest to the center of the contact area. This phenomenon is probably related to the pressure distribution at the contact neck. The pressure usually takes the largest value near the center. A high stress definitely will facilitate dislocation nucleation, and in this way, it is clear why dislocation slip was absent for spherical particles with very small sizes. For very small spheres, the radius of the flat (100) surface near contact neck is not small compared with the particle radius, so the closest step is still moderately far away from the contact center. For instance, for "spherical" nanoparticles with 627 atoms, the shape is indeed quite close to a truncated octahedron.

It seems that surface steps can facilitate the nucleation of partial and perfect dislocations and thereby promoting the dislocation slip mechanism in the collision of nanoparticles. There are two possibilities why dislocation nucleation is accelerated: surface steps can (i) introduce stress intensity, and [16] lower the activation energy of the nucleation. When easy sites for dislocation nucleation are depleted in the nanoparticles, twinning becomes the governing plasticity mechanism. For a flat contact area, once a partial dislocation is nucleated a step of height 1/6[112] is left on the surface. The region around this step would then act as a suitable site for the generation of another Shockley partial. On the other hand, many surfaces steps will hinder

the gliding of partial dislocation on adjacent {111} planes: if two partial dislocations with different Burgers vectors and gliding planes emitted from surface steps meet inside the crystal, a stair-rod dislocation may form and block the further propagation of partials.

4. Discussion

In the present work, we studied the deformation of nanocrystals during collision at different approaching rates at room temperature. The approaching velocities studied included much smaller and much larger values compared with the natural interaction conditions of the two particles. For nanocubes and in general crystals with a shortage of free surface steps, dislocation nucleation is suppressed, and transformation into five-fold twinning may occur by direct geometrical conversion. As discussed before [14], the resultant five-fold twins are metastable structures of the fcc Cu, since each of the five twinned subcrystals are mechanically strained. Such a structure is stabilized for small crystals, however, because of surface energy reduction when {100} faces transforms into {111} phases. For larger crystal sizes, such five-fold twins can be expected to be unstable since the surface energy reduction can no longer offset the mechanical strain energy involved. Experimentally, five-fold twins have indeed been observed in sintered nanoparticles [17]. In our previous work, such five-fold metastable structures can be formed when two Cu nanocrystals coalesce under their own natural interaction conditions driven by free surface elimination [11], or when individual Cu nanocrystals are heated [14]. Here in this study, we further show that these five-fold twins can form as cubic nanocrystals of Cu collide with different rates at room temperature. It is therefore apparent that five-fold twinning by direct geometrical conversion can arise following different triggering means, including heating or mechanical impact of the starting crystal at a wide range of speeds, provided that the crystal does not contain large quantities of surface steps so that dislocation nucleation is suppressed. Also, in our previous work [14], different atomic potentials for Cu were used and the same observation of five-fold twinning was made, indicating that the transformation is a robust conclusion for Cu. However, Table 2 shows that if the approach speed of the two nanocubes is too slow (e.g. 10 m/s), then five-fold twinning will not occur for the crystal size simulated. In the present simulations, the temperature was kept constant at 300K. Higher temperatures may facilitate dislocation nucleation as well as direct geometrical conversion albeit to different extents. So it might be interesting to explore the influence of temperature during the collision of nanocrystals in the future.

The simulation results suggest that high strain rates and small particle sizes facilitate the formation of single twins in spherical nanoparticles. The influence of particle size was elucidated from the geometry and surface steps of the nanospheres, but why high strain rates favor twinning is more difficult to explain. It is well known that high strain rates also promote deformation twinning in coarse-grained and nanocrystalline materials, although the twinning mechanisms in these materials are quite different. For nanocrystals, as discussed in the previous sections, single

twins are formed by partial dislocations nucleated from the particle's free surface. In coarse-grained fcc metals the pole mechanism is operating, and in nanocrystalline materials the main twin mechanism is the sequential emission of partial dislocations from grain boundaries [18]. Since the location of dislocation emission and the actual dislocation mechanism in the twinning process are different, a universal understanding on twinning in these different materials may be difficult to achieve.

The present collision of the two particles falls into the context of contact mechanics except for the nano-scale involved. Adhesive contacts are traditionally described by the JKR model which considers the effect of contact pressure and adhesion inside the area of contact, and the DMT model which assumes that the contact profile remains the same as in Hertzian contact but with additional attractive interactions outside the area of contact [19, 20]. As mentioned above, the present simulated pressure distribution profiles in Fig. 2(b) and 4(b) exhibit an adhesive peak just outside the contact region, and hence the DMT model should provide a better description. We estimate the Tabor coefficient to be around 0.2, which also favors the DMT model [21]. In the DMT model, the total load F comprises the external load and the adhesive force. The adhesive force remains constant throughout the penetration process with magnitude equals to $4\gamma\pi R^*$ (γ: surface energy, R^*: effective sphere radius). For Cu nanoparticles with radius 3.8 nm (25123 atoms), the adhesion by the DMT model is about 4×10^{-3} Dynes. In Fig. 2(a), when two particles are not touching and the external load balances the adhesion, the maximum adhesion is about 2×10^{-3} Dynes and this gets smaller as the two particles come closer. Therefore, the DMT model overestimates the adhesion in our MD simulations.

From now on we neglect the adhesion between the nanoparticles and see how far non-adhesive contact mechanics can take us. Mesarovic and Johnson [22] found from FEM simulations that the pressure distribution in the contact area during the plastic deformation of two non-adhesive spheres is similar to a uniform distribution with magnitude equal to the yield strength of the material. Clearly, Fig. 2(b) shows that the pressure distribution during nanoparticle interaction at the compressive regime is not quite uniform. Besides, the maximum pressure at the contact neck increases as particle size gets larger, in contrary with being fixed yield strength. The Hertzian contact theory therefore seems quite irrelevant to the present study since the strain of the nanoparticles well exceeded the elastic regime. However, the simulation results do show some resemblance. Hertzian contact mechanics predict load (F) to be

$$F = \frac{4}{3}E^*R^{*\frac{1}{2}}d^{\frac{3}{2}},$$

where E^* and R^* are the effective elastic modulus and sphere radius, respectively, and d is the contact depth [20]. For the spherical nanoparticles in our simulations, the reduced load can be expressed as $F' = F/R^{\frac{1}{2}} = \frac{2\sqrt{2}}{3}E^*d^{\frac{3}{2}}$, where R is the particle radius. In Fig. 7 we plot the reduced load (F') vs contact depth at penetration rate 50m/s. Notice that the load at zero

penetration depth is generally less than zero because of the adhesion force. The red curve represents the Hertzian contact prediction with $E^* = 55$GPa, where $\frac{1}{E^*} = 2\frac{1-\nu^2}{E}, E = 100$GPa, and Poisson ratio $\nu = 0.3$. Taking into account adhesion and fluctuations, the MD results conform quite well to the prediction of Hertzian theory. The fact that the elastic Hertzian contact theory can approximately describe the deformation of nanoparticles during their collision is not that surprising. For macroscopic particles indenting one another, dislocation plasticity instantly accommodates the deformation of the material once the yield stress has been reached, as there are ample pre-existing dislocations and dislocation sources. In the nanoparticle case, however, pre-existing dislocations hardly exist and dislocation generation is much more difficult, and so the crystal's deformation can remain elastic up to very large stress and strain approaching the ideal strength limit. In Fig. 2, only very limited dislocation activity is present during the simulated penetration process from 4.4 ps to 20 ps, and so the plastic deformation during this time span is small. After the maximum penetration depth has been reached for $t > 20$ps, the material continues to deform plastically by dislocation slip and the pressure at the contact neck is gradually released.

5. Conclusions

In the present work we have studied the plasticity mechanisms in the room-temperature collision of Cu nanoparticles of different shapes and sizes at different controlled collision rates. We found that twinning was favored in small sized spheres at high collision rates. For cubic particles, single twin formation dominated for larger particle sizes and highly retarded collision rates, but five-fold twin formation via a direct geometrical conversion process took place for small cubic particles with a high proportion of{100} surfaces. The probability for plastic deformation by dislocation slip or twinning is attributed to the availability of surface steps, which act as sources of dislocation nucleation.

Acknowledgement

References

[1] J.R. Greer, W.D. Nix, Physical Review B, 73 (2006) 245410.
[2] R. Maaß, L. Meza, B. Gan, S. Tin, J. Greer, Small, 8 (2012) 1869-1875.
[3] A. Kunz, S. Pathak, J.R. Greer, Acta Materialia, 59 (2011) 4416-4424.
[4] J.R. Greer, J.T.M. De Hosson, Progress in Materials Science, 56 (2011) 654-724.
[5] C.A. Volkert, E.T. Lilleodden, Philosophical Magazine, 86 (2006) 5567-5579.
[6] Z. Shan, R.K. Mishra, S.S. Asif, O.L. Warren, A.M. Minor, Nature materials, 7 (2007) 115-119.
[7] R.M. German, Sintering Theory and Practice, John Wiley & Sons, Inc., 1996.
[8] J.R. Groza, Nanostructured Materials: Processing, Properties, and Applications, (2007).
[9] J.R. Groza, Pergamon Materials Series, 2 (1999) 347-372.
[10] B. Cheng, A.H. Ngan, Computational Materials Science, 74 (2013) 1-11.
[11] B. Cheng, A.H. Ngan, International Journal of Plasticity, (2013).
[12] H.B. Liu, M. José-Yacaman, R. Perez, J.A. Ascencio, Applied Physics A: Materials Science & Processing, 77 (2003) 63-67.
[13] H. Zhu, R.S. Averback, Philosophical Magazine Letters, 73 (1996) 27-33.
[14] B. Cheng, A.H. Ngan, The Journal of chemical physics, 138 (2013) 164314.
[15] H.W. Sheng, M.J. Kramer, A. Cadien, T. Fujita, M.W. Chen, Physical Review B, 83 (2011) 134118.
[16] L. Karkina, I. Karkin, Y. Gornostyrev, Proc. of SPIE, Vol. 7377 (2009) 73770X-73772.
[17] Y.Q. Wang, W.S. Liang, C.Y. Geng, Nanoscale Research Letters, 4 (2009) 684-688.
[18] Y.T. Zhu, X.Z. Liao, X.L. Wu, Progress in Materials Science, 57 (2012) 1-62.
[19] B. Derjaguin, V. Muller, Y.P. Toporov, Journal of Colloid and interface science, 53 (1975) 314-326.
[20] K.L. Johnson, Contact mechanics, Cambridge university press, 1987.
[21] D. Tabor, Journal of Colloid and Interface Science, 58 (1977) 2-13.
[22] S.D. Mesarovic, K. Johnson, Journal of the Mechanics and Physics of Solids, 48 (2000) 2009-2033.

Table 1 – Identified crystal plasticity mechanism during the impact of spherical nanoparticles

Number of atoms in each particle	627	959	1505	3055	10005	25123	40263
10m/s	T	D	D	T+D	D	D	D
50m/s	T	T	T+D	D	D	D	D
200m/s	T	T	T	T+D	D	D	D

Note: "T" denotes twinning, "D" denotes dislocation slip, and "T+D" denotes that both were acting.

Table 2 – Identified crystal plasticity mechanism during the impact of cubic nanoparticles

Number of atoms in each particle	1688	4631	9842	19652	39754
10m/s	T	T	T+D	T	T
50m/s	G	T	T	T	T
200m/s	G	T	T	T	T

Note: "G" denotes formation of fivefold twin via direct geometrical conversion route.

Figure Captions

Fig. 1 – Two free spherical nanoparticles, each with 3055 atoms, colliding upon release from rest.
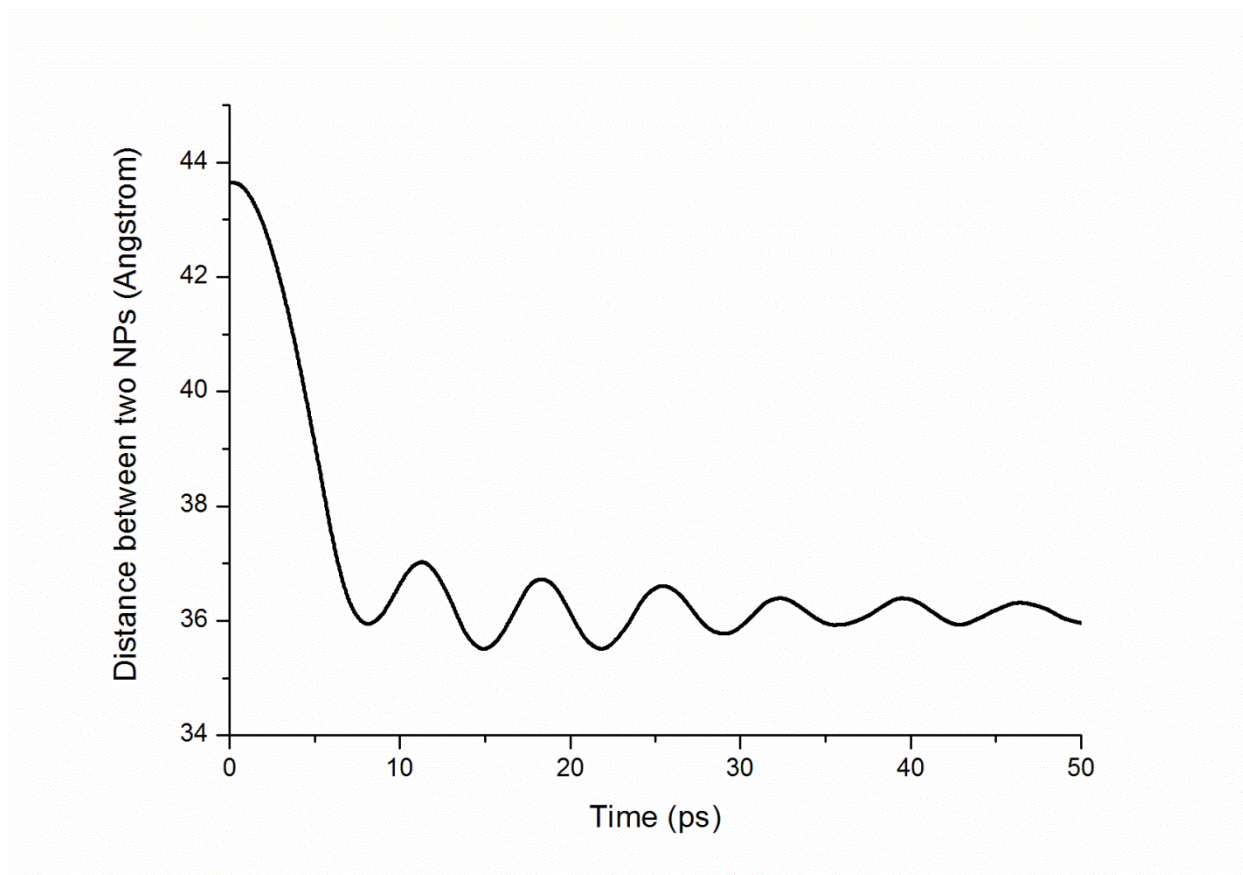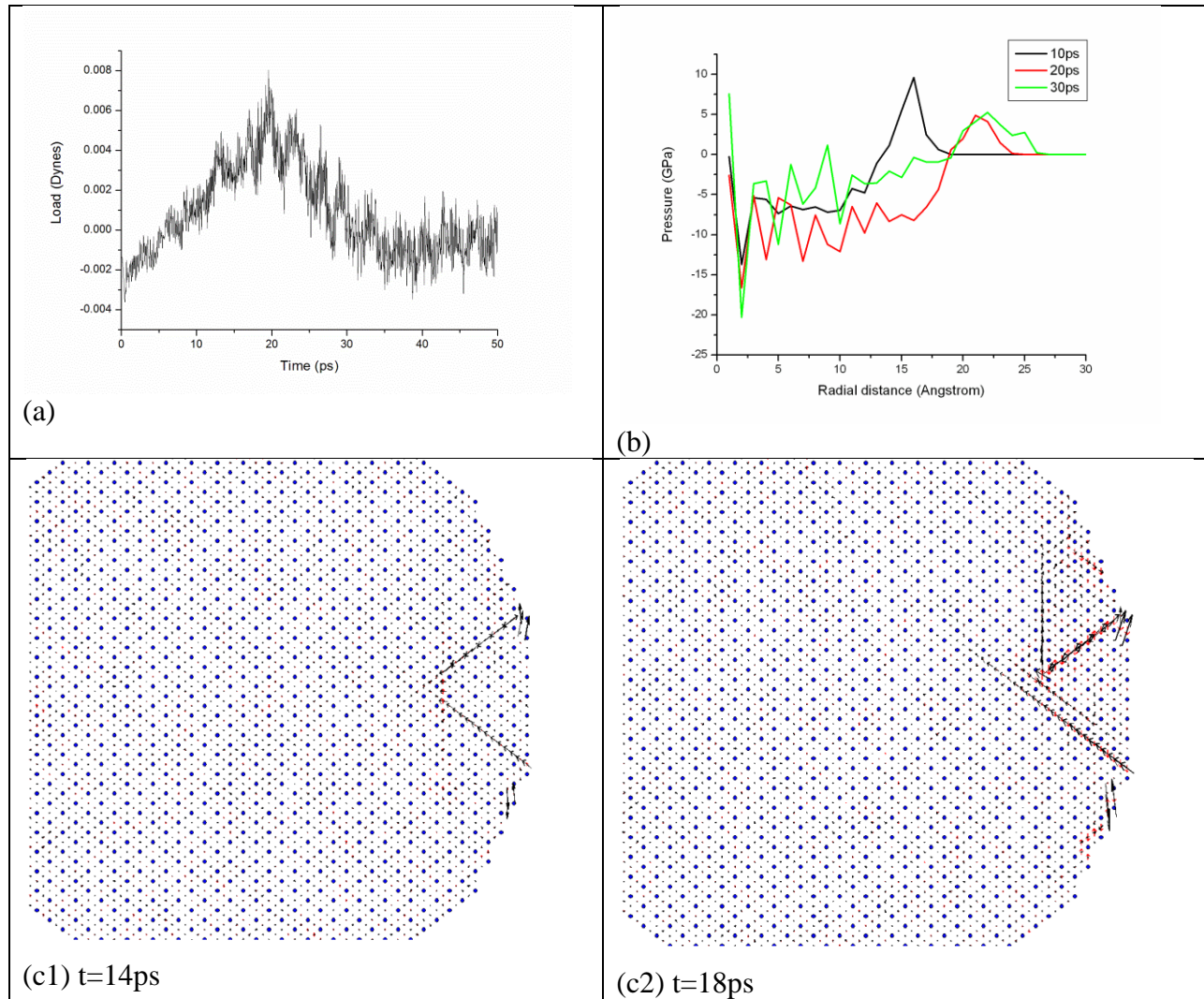
Fig. 2 – Dislocation slip during collision of spherical nanoparticles of 25123 atoms at rate 50m/s. The nanoparticle is collided on from the right hand side of Fig. 2(c).
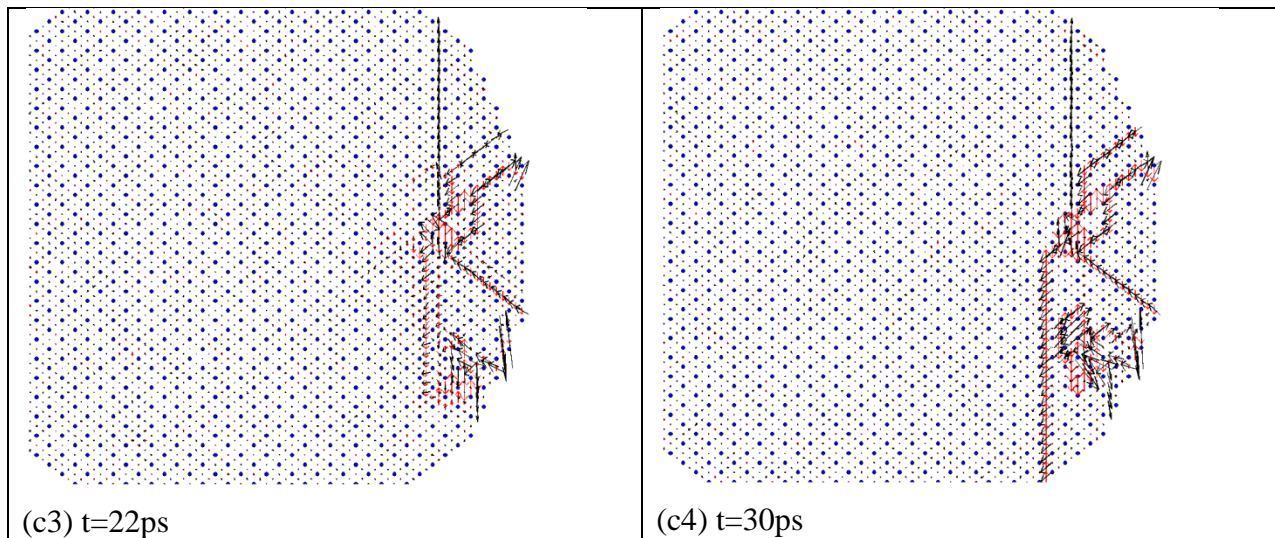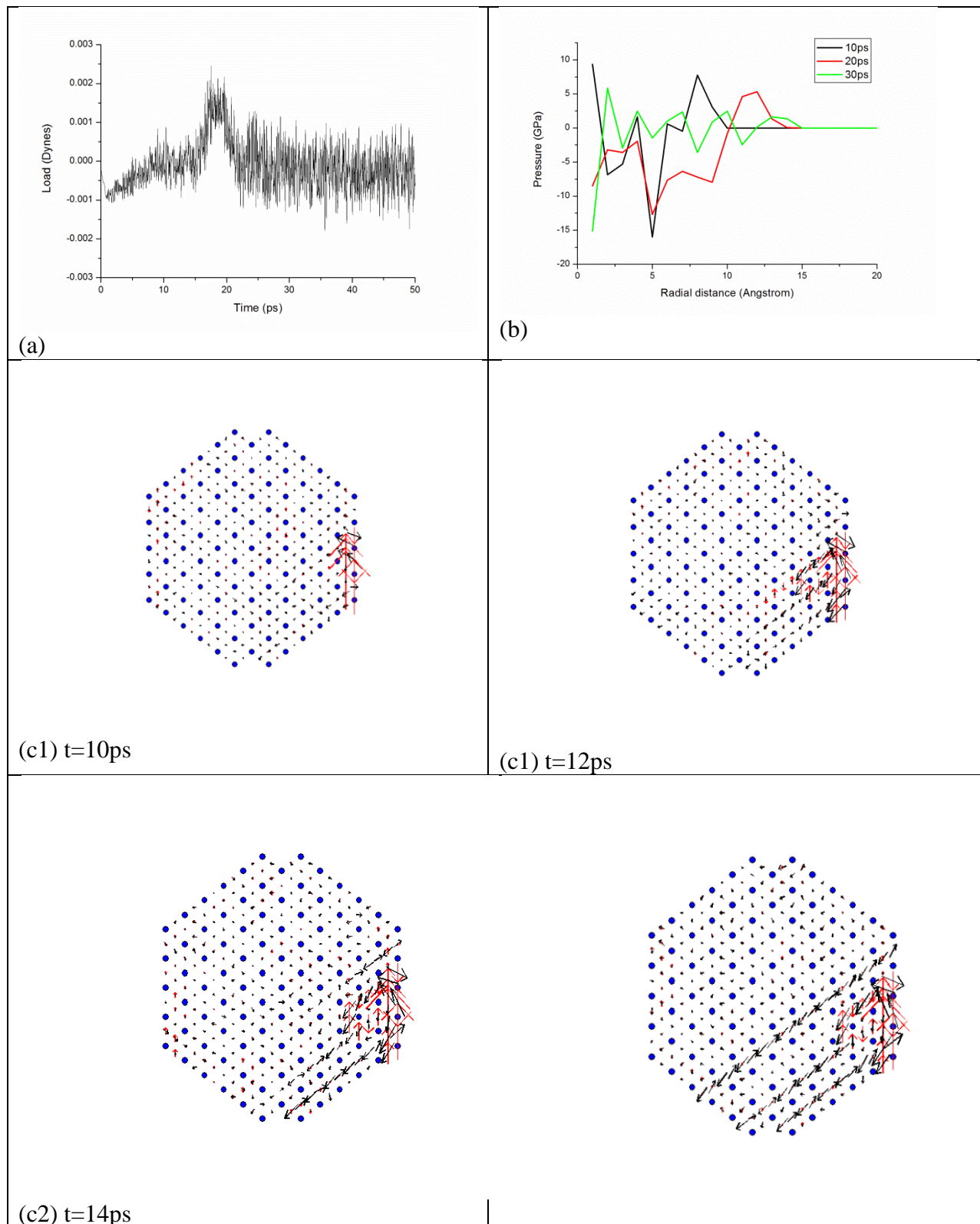
Fig. 3 – Single twinning during collision of spherical particles of 627 atoms at rate 50m/s. The nanoparticle is collided on from the right hand side of Fig. 3(c).

Fig. 4 – Single twinning during collision of cubic particles of 4631 atoms at rate 50m/s. The nanoparticle is collided on from the right hand side of Fig.4(c).

Fig. 5 – The shape transformation of nanoparticles during the direct geometrical conversion process. The penetration rate is 200m/s. The nanoparticle is collided onto from the right hand side. The atoms initially on the edge, diagonal and surfaces of the cube are indicated in green, red and blue, respectively. The final product in (d) is a five-fold twinned structure.

Fig. 6 – The nucleation of dislocations on the surfaces of nanoparticles.

Fig. 7 – The load-contact depth curve of nanoparticle collision simulations. The red curve indicates the theoretical results from Hertzian contact theory.

Fig. 1 – Two free spherical nanoparticles, each with 3055 atoms, colliding upon release from rest.

Fig. 2 – Dislocation slip during collision of spherical nanoparticles of 25123 atoms at rate 50m/s. The nanoparticle is collided on from the right hand side of Fig. 2(c).

(a)

(b)

(c1) t=14ps

(c2) t=18ps

(c3) t=22ps

(c4) t=30ps

Fig. 3 – Single twinning during collision of spherical particles of 627 atoms at rate 50m/s. The nanoparticle is collided on from the right hand side of Fig. 3(c).
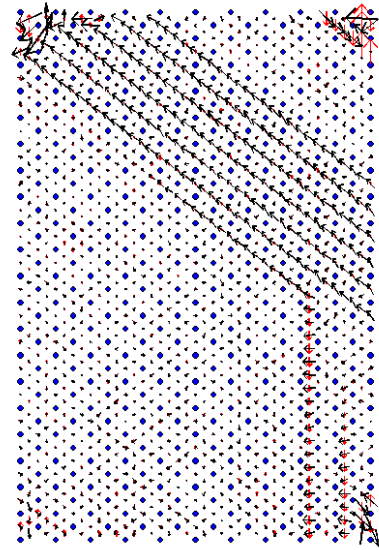

(a)

(b)

(c1) t=10ps

(c1) t=12ps

(c2) t=14ps

	(c3) t=16ps

Fig. 4 – Single twinning during collision of cubic particles of 4631 atoms at rate 50m/s. The nanoparticle is collided on from the right hand side of Fig. 4(c).

(a)

(b)

(c1) t=12ps

(c2) t=14ps
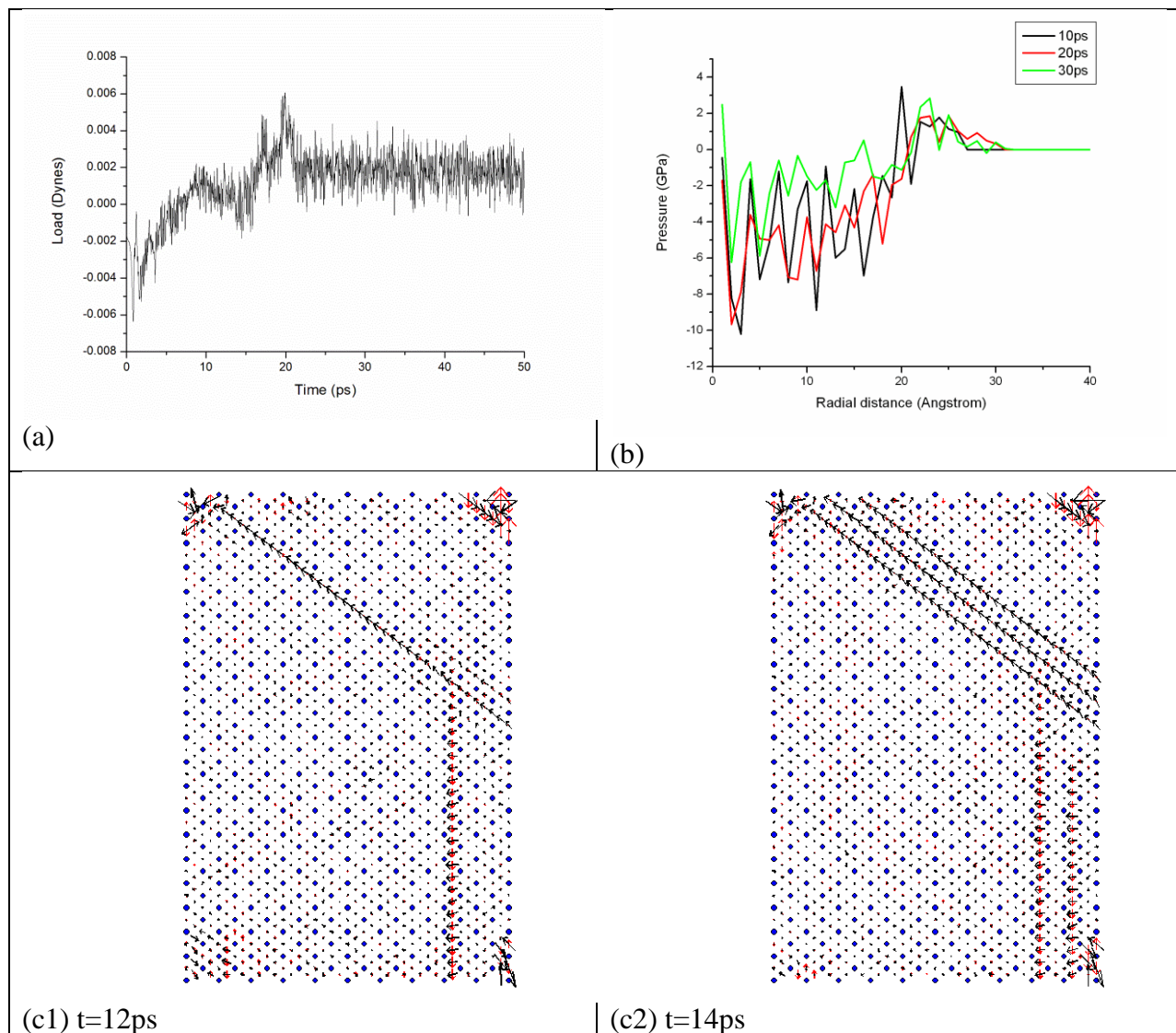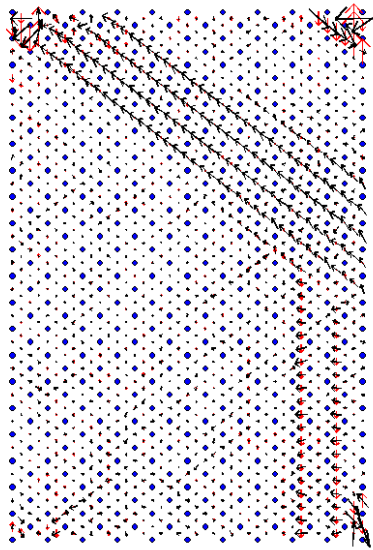
(c3) t=16ps

(c4) t=18ps

Fig. 5 – The shape transformation of nanoparticles during the direct geometrical conversion process. The penetration rate is 200m/s. The nanoparticle is collided onto from the right hand side. The atoms initially on the edge, diagonal and surfaces of the cube are indicated in green, red and blue, respectively. The final product in (d) is a five-fold twinned structure.

(a) t=2ps
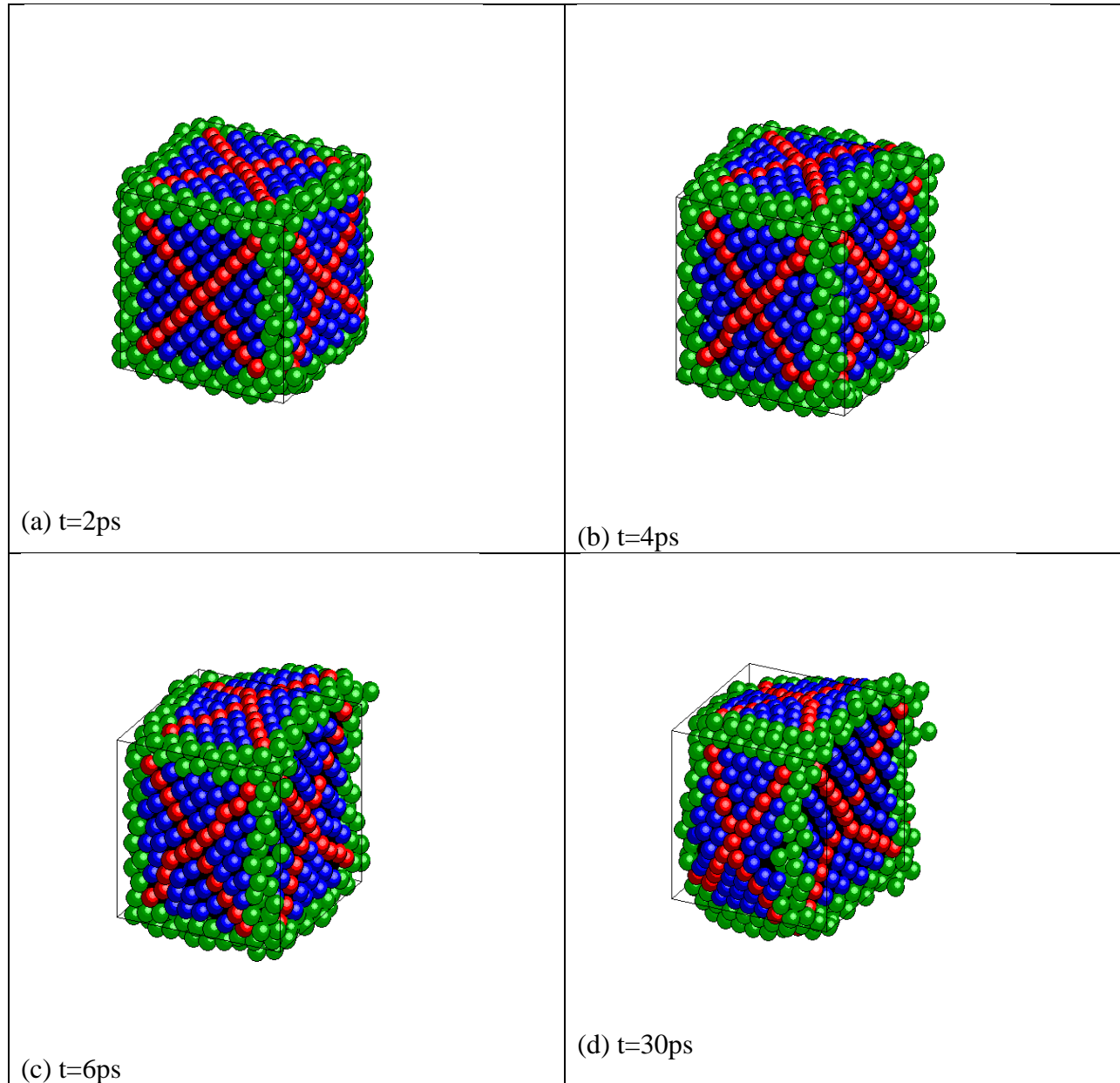
(b) t=4ps

(c) t=6ps

(d) t=30ps

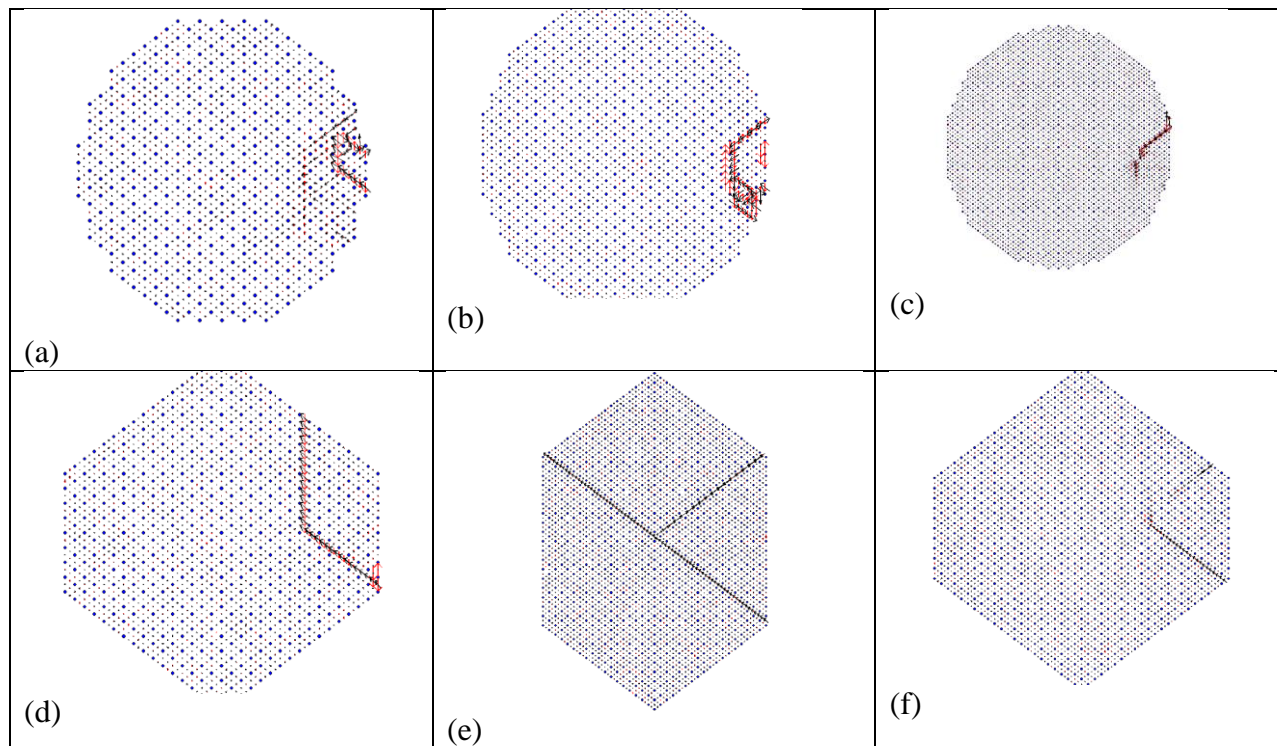Fig. 6 – The nucleation of dislocations on the surfaces of nanoparticles.

Fig. 7 – The load-contact depth curve of nanoparticle collision simulations. The red curve indicates the theoretical results from Hertzian contact theory.